



RESEARCH ARTICLE

Revisiting Old Questions With New Methods: The Effect of Embryonic Motility on Skull Development in the Domestic Chick

Akinobu Watanabe^{1,2,3} 📵 | Izza Arqam¹ | Meredith J. Taylor¹ 📵 | Julia L. Molnar¹

¹New York Institute of Technology, College of Osteopathic Medicine, Old Westbury, New York, USA | ²Division of Paleontology, American Museum of Natural History, New York, New York, USA | ³Life Sciences Department, Natural History Museum, London, UK

Correspondence: Akinobu Watanabe (awatanabe@nyit.edu)

Received: 28 May 2024 | Revised: 11 September 2024 | Accepted: 30 September 2024

Funding: This study was supported by New York Institute of Technology and the U.S. National Science Foundation (Grants DBI 1828305 and IOS 2045466).

Keywords: Gallus | geometric morphometrics | paralysis | plasticity

ABSTRACT

Muscle loading is known to influence skeletal morphology. Therefore, modification of the biomechanical environment is expected to cause coordinated morphological changes to the bony and cartilaginous tissues. Understanding how this musculoskeletal coordination contributes to morphological variation has relevance to health sciences, developmental biology, and evolutionary biology. To investigate how muscle loading influences skeletal morphology, we replicate a classic in ovo embryology experiment in the domestic chick (Gallus gallus domesticus) while harnessing modern methodologies that allow us to quantify skeletal anatomy more precisely and in situ. We induced rigid muscle paralysis in developing chicks mid-incubation, then compared the morphology of the cranium and mandible between immobilized and untreated embryos using microcomputed tomography and landmark-based geometric morphometric methods. Like earlier studies, we found predictable differences in the size and shape of the cranium and mandible in paralyzed chicks. These differences were concentrated in areas known to experience high strains during feeding, including the jaw joint and jaw muscle attachment sites. These results highlight specific areas of the skull that appear to be mechanosensitive and suggest muscles that could produce the biomechanical stimuli necessary for normal hatchling morphology. Interestingly, these same areas correspond to areas that show the greatest disparity and fastest evolutionary rates across the avian diversity, which suggests that the musculoskeletal integration observed during development extends to macroevolutionary scales. Thus, selection and evolutionary changes to muscle physiology and architecture could generate large and predictable changes to skull morphology. Building upon previous work, the adoption of modern imaging and morphometric techniques allows richer characterization of musculoskeletal integration that empowers researchers to understand how tissue-to-tissue interactions contribute to overall phenotypic variation.

1 | Introduction

Understanding the mechanisms of morphological changes is a core mission of evolutionary and developmental biology. While myriad factors influence the formation of individual traits, interactions between structures of different tissue types and developmental origins also play an important role in producing

disparate morphologies within and across species (Atchley and Hall 1991; Gerhart and Kirschner 2007; Woronowicz and Schneider 2019). For example, muscle loading is known to differentially affect bone growth (Wolff 1892; Hogg and Hosseini 1992; Rolfe, Roddy, and Murphy 2013). While this musculoskeletal integration is important for maintaining plasticity in response to injuries and changing environments, it also

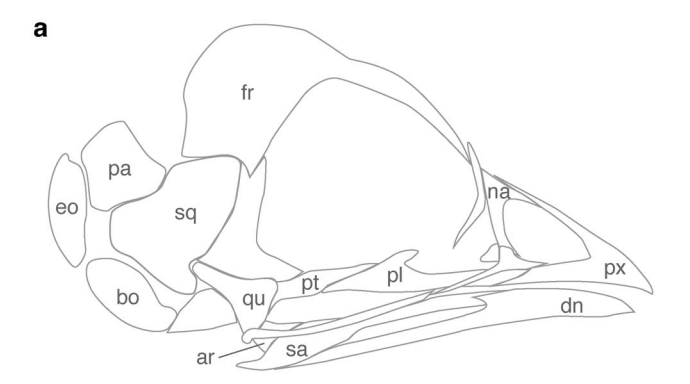
© 2024 Wiley Periodicals LLC.

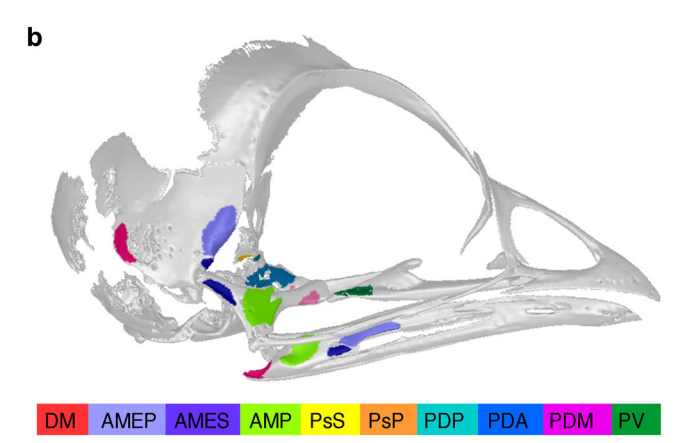
has macroevolutionary implications where evolutionary changes to muscle properties drive coordinated changes in skeletal morphology. Previous experimental work has shown that intermittent muscle contractions during embryonic development change the biomechanical environment in ways that affect skeletal development (Müller and Streicher 1989; Hogg and Hosseini 1992; Müller 2003), including joints (Murray and Drachm 1969) and osteological structures on which muscles attach (Atchley and Hall 1991; Kiliaridis 1995; Murphy and Rolfe 2023). Notably, this mechanism can even produce evolutionary innovations, such as the perching digit in birds (Botelho et al. 2014, 2015) and a species-specific skull element in ducks (Solem et al. 2011; Woronowicz et al. 2018; Woronowicz and Schneider 2019).

For interrogating the effect of muscle loading on bone growth in ovo, the domestic chick (Gallus gallus domesticus) has served as an indispensable model system. Previous studies in chicks have shown that muscle paralysis not only alters muscle properties such as physiological cross-sectional area and fiber orientation (Sullivan 1967; Hall and Herring 1990), but it also inducesmorphological changes in the skull, including differences in bone shape and proportions, reduction in the size of processes for muscle attachment, failure of secondary cartilage formation on membranous bones, and fusion of intercranial joints (Murray and Drachm 1969; Persson 1983; Hall and Herring 1990; Hosseini and Hogg 1991a). Hall and Herring (1990) published a classic paper on in ovo muscle paralysis experiments in the domesticated chick. They injected decamethomium iodide, a neuromuscular blocking agent, during early embryonic stages and harvested embryos in late embryonic stages and shortly before hatching. In their study, Hall and Herring (1990) recorded bone and muscle measurements using wholeembryo clearing and staining followed by dissection of select skeletal elements and muscles. The results showed a marked reduction in the growth of particular bones and muscles in the body, limbs, and head.

Since the publication of these studies, advances in imaging and morphometric techniques have allowed for richer and more precise characterization of anatomical variation. Whereas previous studies quantified skeletal changes in terms of linear and volumetric measurements and weights, the combination of microcomputed tomography (μ CT) imaging with high-density three-dimensional (3D) geometric morphometric methods (e.g., Felice and Goswami 2018; Watanabe et al. 2019) allow for detection of subtle shape differences and intuitive visualization of anatomical differences. This approach permits comprehensive characterization of the shape of many of the individual bones that make up the skull and visualization of areas of the skull with high morphological variation using heat maps.

To investigate how embryonic motility influences skull morphology using these modern techniques, we replicated Hall and Herring's (1990) experiment in muscle paralysis, taking advantage of new methodologies to quantify musculoskeletal anatomy more precisely and comprehensively. Using high-resolution μ CT and high-density geometric morphometrics, we visualize and statistically evaluate the differences in the shape between paralyzed and control embryos. Using these data, we assess whether changes in skull morphologies are concentrated in regions on which jaw muscles attach (Figure 1). The





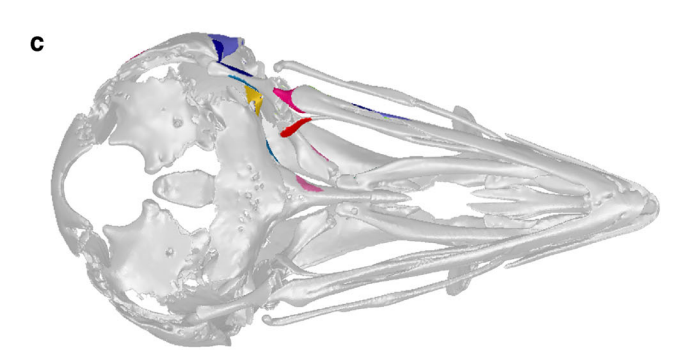


FIGURE 1 | Skull bones and muscle map. Diagrammatic view of skull bones in (a) lateral view and mesh of skull in (b) lateral and (c) ventral views showing attachment areas of jaw muscles. Bone abbreviations (a): articular (ar), basioccipital (bo), dentary (dn), exoccipital (eo), frontal (fr), nasal (na), premaxilla (px), palatine (pl), parietal (pa), pterygoid (pt), quadrate (qu), squamosal (sq), surangular (sa). Muscle abbreviations (b) and (c): adductor mandibulae externus profundus (AMEP), adductor mandibulae externus superficialis (AMES), adductor mandibulae posterior (AMP), depressor mandibulae (DM), pterygoideus dorsalis posterior (PDP), pterygoideus ventralis (PV), pseudotemporalis profundus (PsP), pseudotemporalis superficialis (PSS). [1 column].

rationale is that the mechanism of shape change originates from biomechanical forces generated by individual muscles acting locally at the muscle-bone interface (Woronowicz et al. 2018; Woronowicz and Schneider 2019) rather than a global effect of muscle activity and/or movement. We also expect to see larger changes in the jaw joint, which experiences compressive forces during biting. Finally, we compare shape changes occurring at the developmental scale with avian macroevolutionary trends in craniofacial shape observed in a previous study (Felice and



Goswami 2018). This synthesis of developmental outcomes with evolutionary trends permits investigation into whether evolutionary changes in the skull are concentrated in areas influenced by muscle loading.

2 | Materials and Methods

2.1 | Specimens

Fertilized chicken eggs were provided by the University of Connecticut Poultry Farm and incubated in Ovation 56 EX (Brinsea Products Inc., Titusville, FL, USA) at 37.7°C (99.9°F) at 65% humidity with automated egg rotation. As in previous studies (Hall and Herring 1990), we used decamethomium iodide (Tokyo Chemical Industry America, Portland, OR, USA) as a muscle paralysis agent. At embryonic day (ED) 10, we injected 0.5 mL of 0.2% w/v decamethomium iodide solution in PBS into the air cell after filtering the solution through a 0.45µm syringe filter to remove any undissolved paralysis agent. For the control group, the air cell of eggs was injected with 0.5 mL of PBS and subjected to filtration for consistency in the procedure with the treatment. After injection, both the control and treated eggs were placed back into the incubators with air cells facing up and without rotation. Several embryos in treated eggs did not survive beyond 1-2 days postinjection. These were discarded, and ultimately, our sampling consisted of 24 embryos that reached ED18 stage, split evenly between treatment and control groups (12 in each group). The sampled embryos were rinsed in PBS and placed in 4% paraformaldehyde (PFA) in PBS solution to be stored until CT imaging. The protocol for this study has been approved by IACUC at the New York Institute of Technology, College of Osteopathic Medicine (#2019-AW-01A2; #2023-JM_AW-01).

2.2 | CT Imaging

PFA-fixed embryos were imaged with a Skyscan 1173 micro-CT scanner (Bruker Scientific, Billerica, MA, USA) at the New York Institute of Technology Visualization Center. The scan parameters (Table S1) were determined opportunistically to optimize the overall quality of the scan and available time but did not significantly differ between scanning instances. We imported the CT image stacks into Dragonfly v2021 (Object Research Systems, Montréal, Canada) to segment and create 3-D mesh files of skulls for landmarking. Using GeoMagic Wrap v2020 (3D Systems, Inc., Rock Hill, SC, USA), the cranium and mandible meshes were cleaned (i.e., removal of extraneous elements) and smoothed using its "QuickSmooth" tool.

2.3 | Morphometric Data

2.3.1 | Linear Measurements

We recorded a series of linear distance measurements and angles in Amira v2020.3 (Thermo Fisher Scientific, Waltham, MA, USA) after importing the CT data into the program. These measurements included skull anteroposterior length, skull

mediolateral width, mandible length, mandible width, retroarticular process length, retroarticular process angle, and mandibular angle (Table 1; Figure 2a). As described above, segmentation and 3D reconstructions were performed in Dragonfly.

2.3.2 | Shape Data

The landmark scheme comprises fixed (discrete) landmark points defined anatomically, curve semilandmarks that outline osteological structures, and surface (patch) semilandmarks that characterize the surface topology within skull elements (Figure 2b; Table S2 and S3). We used the program Checkpoint (Stratovan Corporation, Sacramento, CA, USA) to virtually place fixed and curve (semi-)landmarks on skull meshes. Fixed landmarks were placed on both the left and right sides of the skull, whereas curve semilandmarks were manually placed only on the right side. Checkpoint allows any number of points to form a single curve; a feature that allows even complex edges of skull elements to be followed. The fixed and curve landmark data were exported in IDAV Landmark (.pts) format.

In addition to the 24 embryos sampled in this study, we also created an atlas for subsequent patching procedures by placing fixed, curve, and surface semilandmarks on the skull of a more mature, 30-day posthatching chicken. Using R v4.3.1 (R Core Development Team 2023), the coordinate data files were read, and the curves were subsampled using the R package "SURGE" v0.1.0 (https://github.com/rnfelice/SURGE) so that each curve consists of same number of semilandmarks across every specimen. Then, as described by Bardua et al. (2019), we used the "placePatch" function in the "Morpho" package (Schlager 2017) to warp and project the surface semilandmarks of the atlas onto the ED18 skulls. Due to artifacts originating from Procrustes alignment of one-sided data of bilaterally symmetric structures (Cardini 2016, 2017), the curve semilandmarks on the right side of the skull were mirrored across the median plane to generate "left" sided curves before alignment using the "mirrorfill" function in the "paleomorph" R package v0.1.4 (Lucas and Goswami 2022). We performed generalized Procrustes alignment with sliding curve and surface semilandmarks minimizing total bending energy on this bilateral data set. Upon alignment, fixed and curve landmarks on the left sides were removed and shape analysis was performed on the right-sided data only. This resulted in cranium shape data with 52 fixed, 455 curve, and 192 surface (semi-)landmarks. The mandible shape data consisted of 12 fixed, 100 curve, and 90 surface (semi-)landmarks. We did not characterize the position and shape of the articular because it is not rigidly articulated with other mandibular elements, which could affect the overall shape analysis.

2.4 | Analysis

All statistical analysis was conducted in R (R Core Development Team 2023). For linear measurements and angles, we performed ANOVA to test for differences between control and treatment groups. In addition to the raw measurements, we also standardized these values with skull length to evaluate



TABLE 1 | Linear measurements and body weight for control (injected with PBS) and paralyzed (injected with decamethomium iodide, DI) specimens.

		Body	Skull		Mandible			Retroarticular process	
Specimen	Treatment	weight (g)	Length (mm)	Width (mm)	Length (mm)	Width (mm)	Angle (°)	Length (mm)	Angle (°)
2023-001	DI	10.7	26.9	14.0	17.7	8.2	27.6	0.8	151.1
2023-002	DI	6.6	22.0	12.7	14.9	6.6	25.3	0.6	138.5
2023-003	DI	9.3	24.8	13.0	17.0	8.1	28.4	0.7	143.9
2023-004	DI	13.1	27.3	14.7	18.1	8.7	27.7	0.8	136.2
2023-005	DI	10.4	24.2	13.4	16.6	8.0	28.0	0.8	170.1
2023-006	DI	9.6	21.0	12.0	14.4	7.3	29.2	0.8	142.4
2023-007	DI	9.3	24.3	13.6	15.7	6.7	25.3	0.7	153.2
2023-008	DI	10.5	25.1	14.0	16.5	6.9	24.0	0.8	159.3
2023-009	DI	8.6	25.4	13.4	17.4	8.8	25.9	0.8	135.9
2023-010	DI	9.1	24.2	13.5	15.9	6.8	25.9	1.0	161.0
2023-011	DI	11.7	24.6	10.7	18.0	7.5	23.6	0.8	144.3
2023-012	DI	11.4	25.1	13.8	16.7	7.8	26.9	0.6	176.5
2023-076	PBS	23.7	30.1	15.2	20.4	11.5	33.1	1.0	164.3
2023-077	PBS	26.6	30.5	15.4	20.5	11.3	31.6	0.9	154.9
2023-078	PBS	23.7	30.0	14.8	19.8	10.6	31.1	1.2	154.1
2023-079	PBS	23.8	29.9	14.9	20.6	10.7	30.4	0.9	140.3
2023-080	PBS	24.4	30.1	15.0	20.6	10.8	30.6	1.1	149.4
2023-081	PBS	25.7	30.9	15.2	20.9	11.1	31.7	1.0	165.1
2023-082	PBS	22.1	29.5	14.5	20.2	10.5	30.4	1.3	164.8
2023-083	PBS	24.7	30.7	15.2	20.9	11.0	30.3	1.1	159.0
2023-084	PBS	22.3	29.9	14.9	20.0	10.6	30.5	1.0	151.6
2023-085	PBS	22.5	30.4	15.3	20.1	10.5	30.1	1.0	161.3
2023-086	PBS	22.3	29.8	14.3	20.3	10.5	30.3	1.2	164.3
2023-087	PBS	24.7	30.3	15.0	20.0	10.7	32.0	1.6	159.0

 $\it Note:$ See Figure 2 for illustrations of linear measurements recorded in this study.

differences based on proportional morphological changes. For multivariate shape data, we constructed a morphospace based on principal components (PC), calculated total Procrustes variances in each group, visualized shape differences between the control and treatment groups along PC axes as well as heat maps showing localized shape changes, and performed non-parametric MANOVA to explicitly test for shape differences between control and treatment groups.

3 | Results

3.1 | General Observations

Overall, the chicken embryos treated with muscle paralysis agents exhibited consistent morphological differences compared to the control. Notable features of immobilized embryos include a smaller and visibly underdeveloped body, often with hyperflexed or splayed pedal digits. Some immobilized embryos showed severe malformations where the abdomen was open

and fluid-filled. These specimens were discarded and not sampled for this study (i.e., not part of the 24 specimens included in the data). This herniation of the abdominal viscera has been reported previously and is thought to be due to incomplete fusion of the sternum (Hall and Herring 1990; Kablar 2011). Some individual skeletal elements in immobilized embryos showed a reduced amount of articulation with surrounding elements, including less developed articular processes. The CT reconstructions reveal that many of the bones in the cranium and mandible are less ossified in immobilized chicks.

3.2 | Linear and Angular Measurements

With the exception of the retroarticular process angle, all linear measurements and mandibular angles were significantly different between the control and treated chicken embryos (Figure 3). When comparing their body weight, treated embryos showed reduced body weight (Figure 3; $R^2 = 0.956$, p < 0.0001) and greater variance than the control group ($Var_{treatment} = 0.0001$)



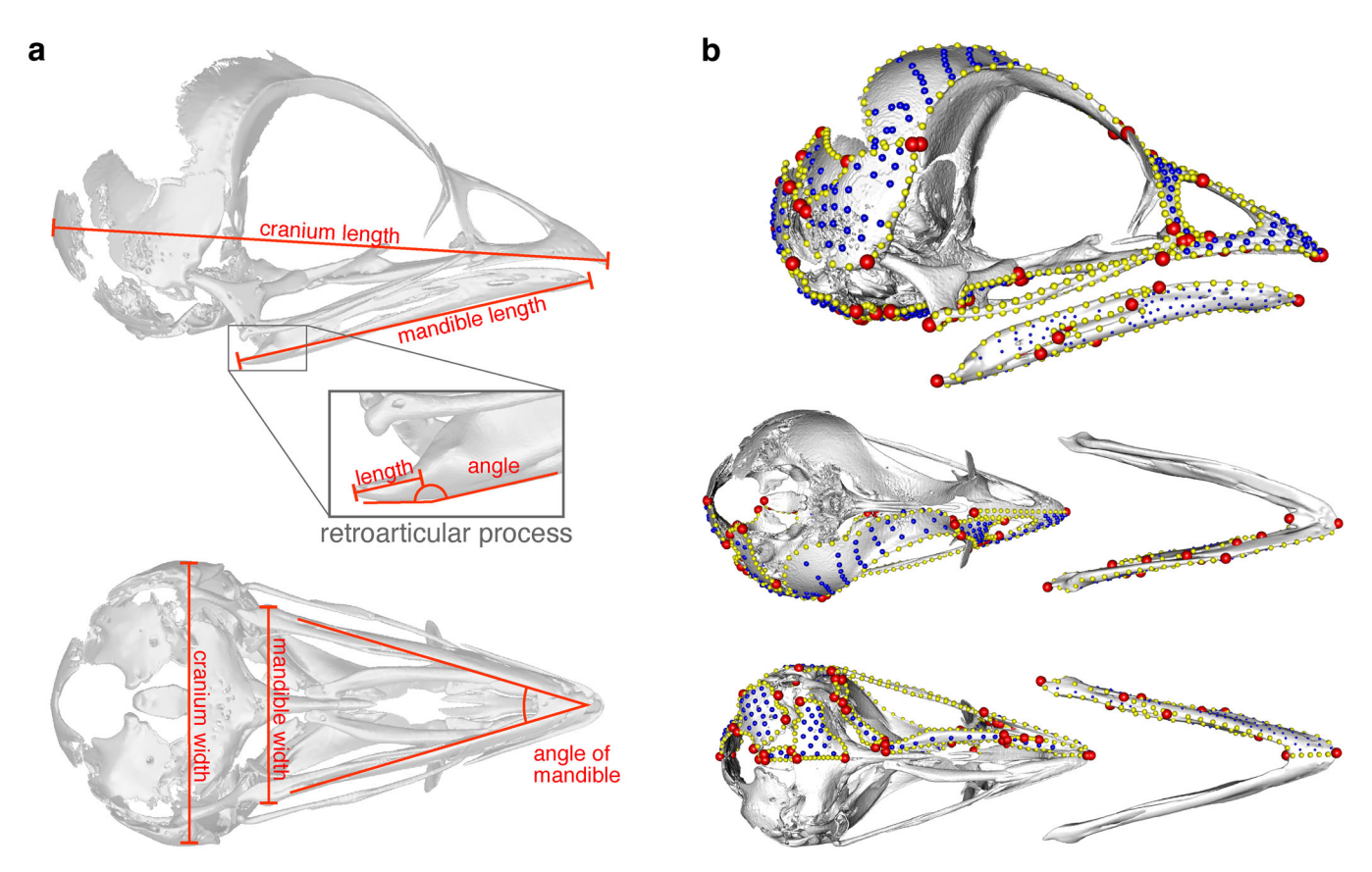


FIGURE 2 | Morphometric data analyzed in this study. (a) Linear and angular measurements are shown on skull reconstruction in anterior (top) and ventral (bottom) views. (b) Landmark scheme shown on skull reconstruction in anterior (top), dorsal (middle), and ventral (bottom) views. [2 columns].

2.802; $Var_{\rm control} = 2.042$). In addition, immobilized chicken embryos showed significantly shorter dimensions for every distance measurement recorded for this study (p < 0.001). The mandibular angle was narrower in treated embryos (p < 0.001). Excluding retroarticular process length, all metrics showed greater variation in immobilized embryos relative to the control.

When comparing percentile decreases in these measurements, we find that mandibular width and retroarticular process length exhibit the greatest mean change from control to treated embryos (29.9% and 37.9%, respectively; Figure 4). Even the variable with the least amount of percentile change, cranial width, showed over 10% change on average. When the linear measurements were standardized by skull length (as proxy for overall size), the morphometric results show that while proportional mandible length did not change significantly $(R^2 < 0.001, p = 0.975)$, the proportional mandibular width was narrower ($R^2 = 0.648$, p < 0.0001), the proportional retroarticular process length was shorter $(R^2 = 0.252,$ p = 0.012), and cranial width was greater relative to length (i.e., relative cranial length was shorter) in treated embryos $(R^2 = 0.410, p = 0.0008)$. Together, the linear and angular measurements demonstrate that embryonic muscle paralysis is associated with smaller and mediolaterally narrower skulls and a pronounced reduction in the retroarticular process. In agreement with previous studies (Murray and Drachm 1969; Hosseini and Hogg 1991a), we also observe that the immobilized chick embryos possess an anteroposteriorly shorter mandible relative to the upper jaw.

3.3 | Shape Data

The morphospace of overall cranial and mandibular shapes shows that treated and control embryos present distinct morphologies (Figure 5). For skull shape, the treated and control embryos separate along PC1 which is associated with dorsoventral depth of the skull, orientation of the upper beak (points more ventrally in immobilized embryos relative to basicranium orientation), and mediolateral breadth, especially in the palate (Figure 5a). Variation along PC2, which is correlated with relative length of the beak, degree of ossification of cranial vault elements, and mediolateral extent of the palate, is greater among skull shape of paralyzed embryos, predominantly driven by specimen 2023-011. The skull of this specimen exhibits more extensive mediolateral compression and less ossification of the cranial vault elements than other embryos in the treatment group. Statistical analysis of shape data, in their original and full dimensionality, demonstrates that the immobilized and control embryos exhibit distinct shapes ($R^2 = 0.33$, p < 0.001). When the shape differences are visualized as a heatmap (Figure 6), we see the greatest difference occurring in the anterior portion of the premaxilla (beak), frontal bone, the posterior portion of the jugal, the dorsal area of the supraoccipital, and the jaw joint.

Similar to skull shape variation, the morphospace of mandible shape also shows distinct shape differences between control and treated chick embryos (Figure 5b). This



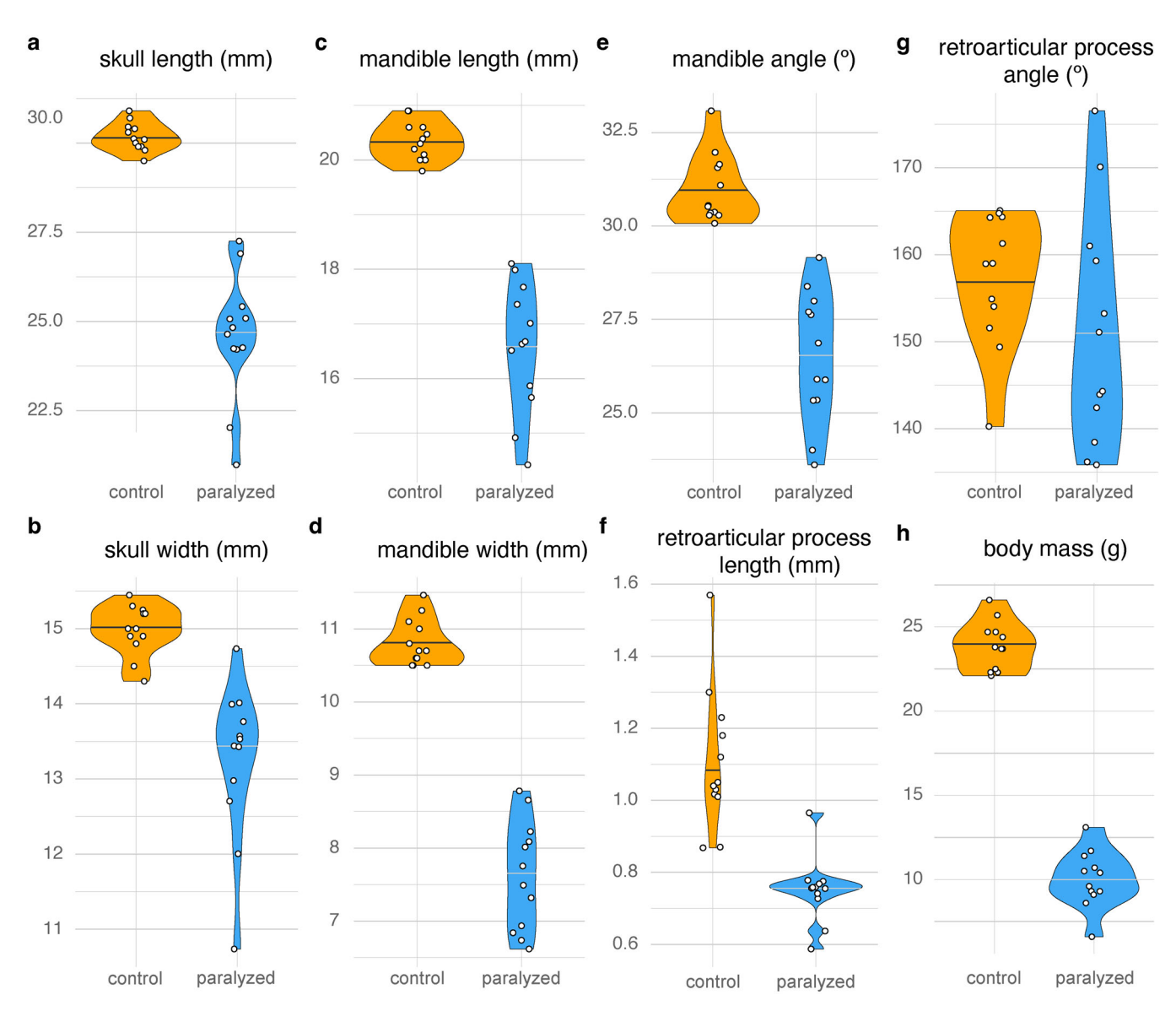


FIGURE 3 | Violin plots of linear and angular measurements, including (a) anteroposterior skull length, (b) mediolateral skull width, (c) anteroposterior mandible length, (d) mediolateral mandible width, (e) mandible angle, (f) retroarticular process length, (g) retroarticular process angle, and (h) body mass. Central line indicates mean value and circles denote measurements of specimens that have been jittered along the horizontal axis. [2 columns].

separation is largely along PC1, which is associated with the relative anteroposterior length of the mandible and a smaller angle between the midline and the orientation of the body of the mandible. PC2 axis accounts for changes in the degree of ossification of elements that form the mandible. MANOVA on full mandibular shape data further verifies that the mandible of paralyzed embryos exhibits distinct shape variation compared to control ($R^2 = 0.427$; p < 0.001). The heatmap of variation at each landmark indicates that the largest differences are concentrated on the anterior tip of the mandible and in the posterior region near the articular surface, which corresponds to the narrower mandibular width in immobilized chicks. The differences in the anterior position of the cranium and mandible are likely due to differences in the anteroposterior extent of the mandible. There are a few regions with elevated differences mid-shaft of the mandible, which results from differences in the degree of ossification of these elements.

4 | Discussion

4.1 | Effect of Mechanical Loading on Skull Morphology

Mechanical forces produced by muscles have been shown to affect the development of the skull, particularly in the areas of jaw articulation and muscle attachment. For example, the development of a coracoid process on the mandible in ducks but not quail is thought to be related to differences in the size and orientation of the jaw adductor muscles (Solem et al. 2011). Furthermore, if duck embryos are paralyzed, the coracoid process fails to form due to a lack of secondary cartilage formation (Solem et al. 2011). Similarly, immobilized mice show reduced coronoid, condylar, and angular processes in the mandible (Kiliaridis 1995; Murphy and Rolfe 2023). Therefore, we predicted that the areas most affected by paralysis would coincide with jaw muscle attachments and articular surfaces, as well as



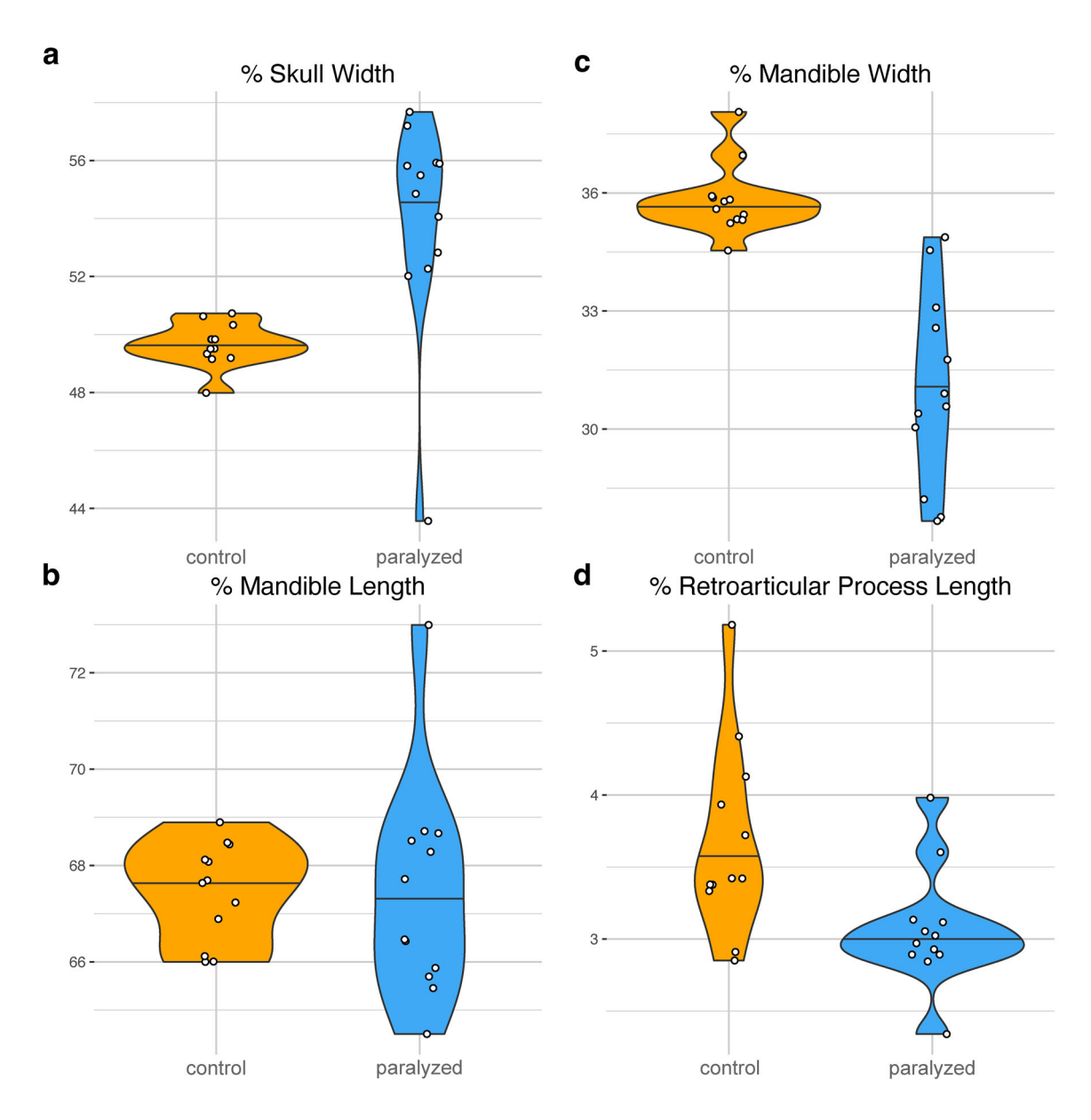


FIGURE 4 | Violin plots of proportional linear measurements corrected by anteroposterior skull length, including proportional (a) mediolateral skull width, (b) anteroposterior mandible length, (c) mediolateral mandible width, and (d) retroarticular process length. Central line indicates mean value, and circles denote measurements of specimens that have been jittered along the horizontal axis. [1 column].

additional regions of the skull that experience high stresses during biting. In the latter prediction, we made the simplifying assumption that the distribution of forces within the skull during embryonic jaw muscle contraction is grossly similar to forces produced during biting in adults. The ideal way to visualize the distribution of forces throughout a complex structure, such as how bite forces are transmitted through the skull, is finite element analysis. Although there is no validated finite element model of a chicken skull during biting, broadly similar patterns of stress distribution have been reported across birds (Degrange et al. 2010; Cuff, Bright, and Rayfield 2015), theropod dinosaurs (Lautenschlager et al. 2013), crocodilians (Porro et al. 2011), and lepidosaurs (Moazen et al. 2009).

As predicted, we observed large shape changes occurred in regions that experience the greatest forces during biting, as well as localized changes near some muscle insertions. The greatest differences between control and paralyzed embryos were in the anterior tip of the premaxilla, dorsal part of the cranium, posterior part of the jugal, posterior section of the mandible, and jaw joint (Figure 6). As bite forces are distributed throughout the cranium, areas of high stress are also found in the posterior portion of the jugal, the premaxilla and nasal bones, and, to a lesser extent, the anterior portion of the frontal bones near their midline contact (Degrange et al. 2010; Cuff, Bright, and Rayfield 2015). Of these three locations, only the nasal lacked large shape differences (Figure 6b). Within the mandible, which generally experiences the highest strains because it transmits most of the bite forces (Lautenschlager et al. 2013), the area between the jaw joint and the adductor insertions experiences high bending stresses (Porro et al. 2011). Large shape differences were present in this area, specifically surrounding the mandibular fenestra and on the ventral edge of the angular (Figure 6a). In addition, when the bite point is in the anterior



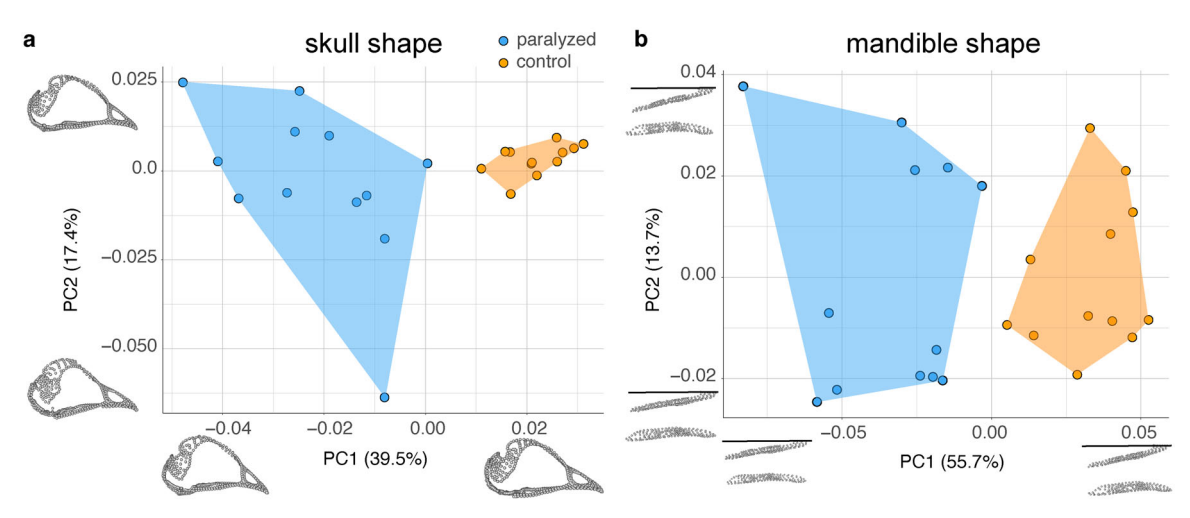


FIGURE 5 | Morphospaces constructed from first two principal components of (a) skull and (b) mandible shape with images showing shape changes along corresponding axes. Mandibles are shown in dorsal (top) and right lateral (bottom) orientations. Note the separation in distribution of shapes between paralyzed and control embryos. [2 columns].

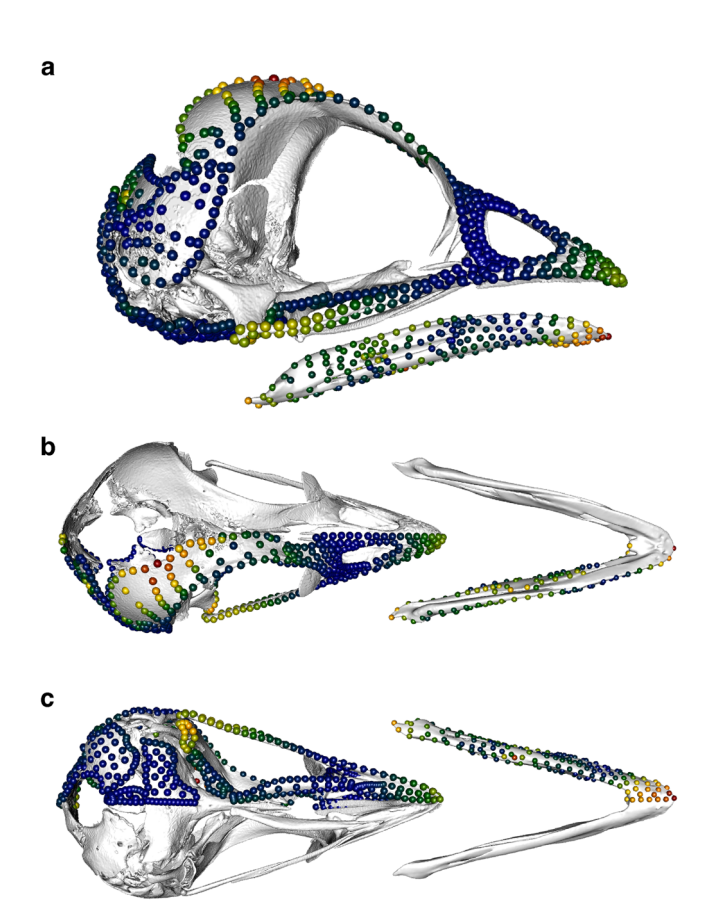


FIGURE 6 | Heat-map showing the degree of regional shape differences between mean shapes of immobilized and control embryos, where warmer colors denote greater Procrustes difference. Skull and mandible are shown in (a) lateral, (b) dorsal, and (c) ventral views. Skull shape differences are concentrated in the jugal, frontal, jaw joint, and anterior portion of the premaxilla. In the mandible, the shape differences are concentrated in the anterior tip, retroarticular process, and the margins of the mandibular canal. [1 column].

part of the jaw, a peak in stress occurs at the tip of the beak (Degrange et al. 2010) which agrees with shape changes concentrated at the anterior tip of the premaxilla. The jaw joint experiences high compressive forces during biting that become distributed throughout the skull and mandible (Degrange et al. 2010; Porro et al. 2011; Cuff, Bright, and Rayfield 2015). The jaw joint is made up of the quadrate, which experienced large shape changes (Figure 6c), and the articular, which we did not measure (see Section 2.3.2). The shape difference at this joint could be attributed to a lack of concavity on the articulating surface, as has been reported previously (Murray and Drachman 1969; Persson 1983). Another factor contributing to shape differences could be that the joints are areas typically characterized by contribution from secondary cartilage, which has been shown to be absent in immobilized embryos (Murray and Drachm 1969).

During biting, localized areas of high tensile stress are found near muscle attachments, particularly those of the adductor muscles which are the main contributors to bite force (Lautenschlager et al. 2013). Of the bones we measured, origins of adductors are present on the lateral aspect of the squamosal (AMES, AMEM, AMEP) and quadrate (AMES, AMP) (Holliday and Witmer 2007; Cost et al. 2022) (in some birds AMEP attaches to the parietal, but we did not observe this attachment). As mentioned above, the quadrate showed high shape variability. Surprisingly, the squamosal, where some of the jaw adductors attach, showed low shape variability (Figure 6a,c), possibly because it ossifies relatively early in development (see below) and may thus be less susceptible to mechanical forces that are exerted later in development. In the mandible, areas of high shape variability were found near insertions of the AMES (dorsal edge of mid-shaft of the mandible) and DM (retroarticular process) (Figure 6a,c). Collectively, these results indicate that attachment points of muscles are areas of concentrated morphological changes under differing muscle loadings.



With the use of muscle paralysis agents, it is worth considering that the effect of skeletal muscles on skeletal development is not completely eliminated because static loading is still exerted. Total elimination of this factor would be achieved through the use of specific genetic lines, such as a mouse line that lacks *Myf5*, *Mrf4*, and *MyoD* resulting in embryos that lack any skeletal muscles (e.g., Rot-Nikcevic et al. 2006; Kablar 2011). However, these mouse lines show congruent outcomes as paralysis experiments, including reduced angular process and changes in the region of the coronoid process. As such, the results of our study are expected to mirror the morphological changes expected from outcomes of complete loss of skeletal muscles.

4.2 | Developmental and Evolutionary Implications

While an extensive body of work exists on the developmental interplay between muscles and bones, a precise mechanistic understanding of how loading contributes to the proliferation of ossified, as well as cartilaginous, tissue has remained challenging (Hosseini and Hogg 1991b; Nowlan, Murphy, and Prendergast 2008; Nowlan et al. 2010; Murphy and Rolfe 2023). Previous experiments on mouse and chick models have demonstrated that a multitude of factors are involved in musculoskeletal integration. For example, mechanical loading is known to participate in *Wnt* signaling pathway (Murphy and Rolfe 2023), expression of *IGF-I* production (Bikle 2008), and *FGF* as well as *TGF-beta* signaling (Woronowicz et al. 2018). In addition, cranial neural crest cells are also likely involved due to their importance in both bone and muscle formation (Tokita and Schneider 2009; Herring 2011).

Our results show that the greatest shape differences occur on bones that are derived from neural crest cells, including the beak (premaxilla), jugal, and frontal bones. Although neural crest cells could be a possible cause for this result, not all neural crest-derived bones undergo substantial morphological changes. In addition, there is no evidence that bones derived from neural crest cells respond differently from mechanical forces compared to other bones. Another consideration is that neural crest-derived bones generally undergo ossification later than primary endochondral bones in the basicranium, which is not derived from neural crest cells. As such, the timing of ossification relative to muscle development is likely a critical factor, rather than being a derivative of neural crest cells, in determining the differential magnitude of musculoskeletal integration throughout the skull.

We may expect that bones that continue to ossify after adjacent muscles begin to contract would be most affected by induced paralysis. However, in their chick paralysis experiment, Hall and Herring (1990) found the clavicle, which is one of the earliest forming bones, to be the most deformed in immobilized embryos. Even close spatial association of bone to muscle does not account for the differential effect of muscle paralysis on bone morphology. For instance, the squamosal bone, where jaw adductor muscles attach, exhibits similar morphologies between immobilized and control groups. Similarly, when examining cichlid species, Conith, Lam, and Albertson (2019)

found mixed results on how skeletal variation is associated with muscle attachment points. Their results suggest that the effect of muscle loading propagates beyond bones on which muscles attach, where mechanical loading is transmitted across adjacent bones (Herring 1993).

With the use of modern imaging and morphometric techniques, our results are consistent with previous studies that show predictable plastic changes in skeletal morphology due to muscle paralysis. Although this plasticity undoubtedly contributes to variation within species, the shape differences we observe between control and paralyzed embryos could potentially extend to macroevolutionary patterns. Muscle properties and their attachment points are expected to be under strong selection (e.g., jaw adduction for feeding). Therefore, these experimental embryological studies illuminate regions of the skull that are robust or particularly susceptible to evolutionary changes in muscle loading from natural selection. High-density geometric morphometric data of the cranium across the avian phylogeny have shown that the rostrum (including the premaxilla and jugal) and the cranial vault (including the frontal) are regions that show high disparity and elevated rates of shape evolution (Felice and Goswami 2018). These cranial regions that show extensive evolutionary changes correspond to areas that show the largest differences between immobilized and control embryos (Figure 6). Although it would be difficult to isolate its cascading effects on skull morphology, selection on biomechanical properties of cranial muscles has likely contributed to how the skull has evolved.

4.3 | Future Directions

The central aim of this study was to experimentally investigate the effect of embryonic muscle contractions on skull development using modern imaging and morphometric techniques. Compared to classic methods by which this study is inspired, imaging modalities, such as µCT imaging, allow for in situ anatomical data at high resolution. For instance, µCT has been used to measure the degree of mineralization in mice lines that lack skeletal muscles (Gomez et al. 2007). In addition to µCT imaging, modern morphometric approaches, particularly geometric morphometrics, provide a powerful quantitative framework to characterize, visualize, and statistically evaluate morphological variation. This study focused on craniofacial and mandibular shapes, but the method can easily be extended to include the postcranial skeleton where we would expect to see notable differences. In fact, previous studies have shown that embryonic muscle contractions lead to the emergence of new morphological traits (e.g., Botelho et al. 2015; Hall 2009 in Murphy and Rolfe 2023). Beyond skeletal anatomy, current staining and imaging techniques, such as diffusible-iodine contrast-enhanced (dice) CT (Metscher 2009a, 2009b; Gignac and Kley 2014; Gignac et al. 2016), would allow for muscle architecture and other soft tissue anatomy to be reconstructed in situ. Such data would permit assessment of the effect of paralysis on muscle properties (e.g., volume, length, and number of fascicles) that ultimately lead to skeletal changes. Moreover, sampling earlier embryonic stages and postnatal individuals would allow investigations on the timing and duration of these interactions and how they shape the adult phenotype.



Previous studies sampling multiple stages of the domestic chick have shown that the onset of ossification is not altered by muscle paralysis (Hosseini and Hogg 1991a). Furthermore, additional phenotypic responses, namely morphological asymmetry, would inform the severity of dysmorphology resulting from the absence or restricted loading during skeletogenesis, which has been reported for the mandible by Hall and Herring (1990). Together with the strength of experimental developmental research to infer causation, these modern techniques collectively permit a more holistic investigation into how interactions between different tissue types ultimately result in the adult form within or across taxa.

5 | Conclusions

Employing μ CT imaging and modern morphometric methods, we find that muscle paralysis generates predictable changes to skull morphology that are consistent with the findings of previous studies. In addition to an overall reduction in size and mediolaterally narrower skull, these morphological changes are concentrated in the shape of the beak tip, skull roof, and areas around the jaw joint. These results align with the expectation that areas of muscle attachment and functional significance are susceptible to muscle action and inaction. Furthermore, localized areas of the skull that undergo the greatest morphological changes generally correspond with those that exhibit the highest degree of interspecific variation across birds (Felice and Goswami 2018), suggesting that macroevolutionary trends in skull evolution may have, at least partly, emerged through selection on biomechanical properties of cranial muscles.

Understanding musculoskeletal interactions has important implications for not only evolutionary and developmental biology, but also for human musculoskeletal diseases (e.g., De Vries and Fong 2007; Shea, Rolfe, and Murphy 2015), athletics (Suominen 2006), and disuse for clinical applications and space travel (Sibonga et al. 2007). Through this study, we provide an example of modern approaches to investigate this critical and complex phenomenon that could easily be applied across a broad taxonomic spectrum. As Herring (1993) stated, "A primary need is to extend the range of species studied experimentally to include fishes, amphibians, and reptiles and birds other than the omnipresent chick embryo."

Acknowledgments

We thank Robert Durzinky, Rebecca German, Anthony Herrel, and Matthias Starck for organizing the "Symposium in honor of Sue Herring: a giant in her field" at the 2023 International Congress of Vertebrate Morphology conference in Cairns, Australia, and for inviting us to contribute to this special issue. Naturally, we are indebted to Sue Herring for her profound contributions to the field that inspired this study. We also thank Mary Margaret Cole and Lisa Nowak (University of Connecticut Poultry Unit) for their assistance in supplying fertilized eggs, Kelsi Hurdle (New York Institute of Technology Visualization Center) for μ CT imaging, Comet Technologies Canada (Montréal, Canada) for providing free noncommercial licensing for Dragonfly, organizers and instructors of the Marine Biological Laboratory (Woods Hole, Massachusetts) summer embryology course in 2019 for providing training and funding to learn embryology techniques (to Akinobu Watanabe), and two anonymous reviewers who provided constructive feedback on an earlier version of the

manuscript that helped improve the article. U.S. National Science Foundation (DBI 1828305 to Julia L. Molnar; IOS 2045466 to Akinobu Watanabe) and the New York Institute of Technology provided funding for this research.

Conflicts of Interest

The authors declare no conflicts of interest.

Peer Review

The peer review history for this article is available at https://www.webofscience.com/api/gateway/wos/peer-review/10.1002/jmor.21785.

Data Availability Statement

The data that supports the findings of this study are available in the supplementary material of this article on Data Dryad: https://doi.org/10.5061/dryad.905qftttn.

References

Atchley, W. R., and B. K. Hall. 1991. "A Model for Development and Evolution of Complex Morphological Structures." *Biological Reviews* 66: 101–157.

Bardua, C., R. N. Felice, A. Watanabe, A.-C. Fabre, and A. Goswami. 2019. "A Practical Guide to Sliding and Surface Semilandmarks in Morphometric Analyses." *Integrative Organismal Biology* 1, no. 1: obz016. https://doi.org/10.1093/iob/obz016.

Bikle, D. D. 2008. "Integrins, Insulin Like Growth Factors, and the Skeletal Response to Load." *Osteoporosis International* 19: 1237–1246.

Botelho, J. F., D. Smith-Paredes, D. Nuñez-Leon, S. Soto-Acuña, and A. O. Vargas. 2014. "The Developmental Origin of Zygodactyl Feet and Its Possible Loss in the Evolution of Passeriformes." *Proceedings of the Royal Society B: Biological Sciences* 281: 20140765. https://doi.org/10.1098/rspb.2014.0765.

Botelho, J. F., D. Smith-Paredes, S. Soto-Acuñ, J. Mpodozis, V. Palma, and A. O. Vargas. 2015. "Skeletal Plasticity in Response to Embryonic Muscular Activity Underlies the Development and Evolution of the Perching Digit of Birds." *Scientific Reports* 5: 1–11.

Cardini, A. 2016. "Lost in the Other Half: Improving Accuracy in Geometric Morphometric Analyses of One Side of Bilaterally Symmetric Structures." *Systematic Biology* 65, no. 6: 1096–1106. https://doi.org/10.1093/sysbio/syw043.

Cardini, A. 2017. "Left, Right or Both? Estimating and Improving Accuracy of One-Side-Only Geometric Morphometric Analyses of Cranial Variation." *Journal of Zoological Systematics and Evolutionary Research* 55, no. 1: 1–10. https://doi.org/10.1111/jzs.12144.

Conith, A. J., D. T. Lam, and R. C. Albertson. 2019. "Muscle-Induced Loading as an Important Source of Variation in Craniofacial Skeletal Shape." *Genesis* 57, no. 1: e23263.

Cost, I. N., K. C. Sellers, R. E. Rozin, A. T. Spates, K. M. Middleton, and C. M. Holliday. 2022. "2D and 3D Visualizations of Archosaur Jaw Muscle Mechanics, Ontogeny and Phylogeny Using Ternary Diagrams and 3D Modeling." *Journal of Experimental Biology* 225: jeb243216.

Cuff, A. R., J. A. Bright, and E. J. Rayfield. 2015. "Validation Experiments on Finite Element Models of an Ostrich (*Struthio camelus*) Cranium." *PeerJ* 3: e1294. https://doi.org/10.7717/peerj.1294.

Degrange, F. J., C. P. Tambussi, K. Moreno, L. M. Witmer, and S. Wroe. 2010. "Mechanical Analysis of Feeding Behavior in the Extinct "Terror Bird" *Andalgalornis steulleti* (Gruiformes: Phorusrhacidae)." *PLoS One* 5, no. 8: e11856.

De Vries, J. I. P., and B. F. Fong. 2007. "Changes in Fetal Motility as a Result of Congenital Disorders: An Overview." *Ultrasound in Obstetrics & Gynecology* 29, no. 5: 590–599.



Felice, R. N., and A. Goswami. 2018. "Developmental Origins of Mosaic Evolution in the Avian Cranium." *Proceedings of the National Academy of Sciences* 115, no. 3: 555–560. https://doi.org/10.1073/pnas. 1716437115.

Gerhart, J., and M. Kirschner. 2007. "The Theory of Facilitated Variation." Proceedings of the National Academy of Sciences 104: 8582–8589.

Gignac, P. M., and N. J. Kley. 2014. "Iodine-Enhanced Micro-CT Imaging: Methodological Refinements for the Study of the Soft-Tissue Anatomy of Post-Embryonic Vertebrates." *Journal of Experimental Zoology Part B: Molecular and Developmental Evolution* 322, no. 3: 166–176. https://doi.org/10.1002/jez.b.22561.

Gignac, P. M., N. J. Kley, J. A. Clarke, et al. 2016. "Diffusible Iodine-Based Contrast-Enhanced Computed Tomography (diceCT): An Emerging Tool for Rapid, High-Resolution, 3-D Imaging of Metazoan Soft Tissues." *Journal of Anatomy* 228, no. 6: 889–909. https://doi.org/10.1111/joa.12449.

Gomez, C., V. David, N. M. Peet, et al. 2007. "Absence of Mechanical Loading in Utero Influences Bone Mass and Architecture but Not Innervation in Myod-Myf5-Deficient Mice." *Journal of Anatomy* 210, no. 3: 259–271.

Hall, B. K., and S. W. Herring. 1990. "Paralysis and Growth of the Musculoskeletal System in the Embryonic Chick." *Journal of Morphology* 206: 45–56. https://doi.org/10.1002/jmor.1052060105.

Hall, J. G. 2009. "Pena-Shokeir Phenotype (Fetal Akinesia Deformation Sequence) Revisited." *Birth Defects Research Part A: Clinical and Molecular Teratology* 85, no. 8: 677–694.

Herring, S. W. 1993. "Formation of the Vertebrate Face: Epigenetic and Functional Influences." *American Zoologist* 33: 472–483.

Herring, S. W. 2011. "Muscle-Bone Interactions and the Development of Skeletal Phenotype." In *Epigenetics: Linking Genotype and Phenotype in Development and Evolution*, edited by B. Hallgrimsson and B. K. Hall, 221–237. Berkeley/Los Angeles, California: University of California Press.

Hogg, D. A., and A. Hosseini. 1992. "The Effects of Paralysis on Skeletal Development in the Chick Embryo." *Comparative Biochemistry and Physiology Part A: Physiology* 103: 25–28.

Holliday, C. M., and L. M. Witmer. 2007. "Archosaur Adductor Chamber Evolution: Integration of Musculoskeletal and Topological Criteria in Jaw Muscle Homology." *Journal of Morphology* 268: 457–484. https://doi.org/10.1002/jmor.10524.

Hosseini, A., and D. A. Hogg. 1991a. "The Effects of Paralysis on Skeletal Development in the Chick Embryo. I. General Effects." *Journal of Anatomy* 177: 159–168.

Hosseini, A., and D. A. Hogg. 1991b. "The Effects of Paralysis on Skeletal Development in the Chick Embryo. II. Effects on Histogenesis of the Tibia." *Journal of Anatomy* 177: 169–178.

Kablar, B. 2011. "Role of Skeletal Muscles in the Epigenetic Shaping of Organs, Tissues, and Cell Fate Choices." In *Epigenetics: Linking Genotype and Phenotype in Development and Evolution*, edited by B. Hallgrímsson and B. K. Hall, 256–268. Berkeley/Los Angeles, California: University of California Press.

Kiliaridis, S. 1995. "Masticatory Muscle Influence on Craniofacial Growth." *Acta Odontologica Scandinavica* 53, no. 3: 196–202.

Lautenschlager, S., L. M. Witmer, P. Altangerel, and E. J. Rayfield. 2013. "Edentulism, Beaks, and Biomechanical Innovations in the Evolution of Theropod Dinosaurs." *Proceedings of the National Academy of Sciences* 110: 20657–20662.

Lucas, T., and A. Goswami. 2022. Package 'paleomorph' v0.1.4. https://github.com/timcdlucas/paleomorph/.

Metscher, B. D. 2009a. "MicroCT for Comparative Morphology: Simple Staining Methods Allow High-Contrast 3D Imaging of Diverse

Non-Mineralized Animal Tissues." *BMC Physiology* 9, no. 11: 1–14. https://doi.org/10.1186/1472-6793-9-11.

Metscher, B. D. 2009b. "MicroCT for Developmental Biology: A Versatile Tool for High-Contrast 3D Imaging at Histological Resolutions." *Developmental Dynamics* 238, no. 3: 632–640. https://doi.org/10.1002/dvdy.21857.

Moazen, M., N. Curtis, P. O'Higgins, S. E. Evans, and M. J. Fagan. 2009. "Biomechanical Assessment of Evolutionary Changes in the Lepidosaurian Skull." *Proceedings of the National Academy of Sciences* 106, no. 20: 8273–8277.

Müller, G. B. 2003. "Embryonic Motility: Environmental Influences and Evolutionary Innovation." *Evolution & Development* 5: 56–60.

Müller, G. B., and J. Streicher. 1989. "Ontogeny of the Syndesmosis Tibiofibularis and the Evolution of the Bird Hindlimb: A Caenogenetic Feature Triggers Phenotypic Novelty." *Anatomy and Embryology* 179: 327–339.

Murphy, P., and R. A. Rolfe. 2023. "Building a Co-Ordinated Musculoskeletal System: The Plasticity of Developing Skeleton in Response to Muscle Contractions." In *Roles of Skeletal Muscle in Organ Development: Prenatal Interdependence among Cells, Tissues, and Organs*, edited by B. Kabler, 81–110. Cham, Switzerland: Springer Nature.

Murray, P. D. F., and D. B. Drachm. 1969. "The Role of Movement in the Development of Joints and Related Structures: The Head and Neck in the Chick Embryo." *Development* 22: 349–371. https://doi.org/10.1242/dev.22.3.349.

Nowlan, N. C., P. Murphy, and P. J. Prendergast. 2008. "A Dynamic Pattern of Mechanical Stimulation Promotes Ossification in Avian Embryonic Long Bones." *Journal of Biomechanics* 41, no. 2: 249–258.

Nowlan, N. C., J. Sharpe, K. A. Roddy, P. J. Prendergast, and P. Murphy. 2010. "Mechanobiology of Embryonic Skeletal Development: Insights From Animal Models." *Birth Defects Research Part C: Embryo Today: Reviews* 90, no. 3: 203–213.

Persson, M. 1983. "The Role of Movements in the Development of Sutural and Diarthrodial Joints Tested by Long-Term Paralysis of Chick Embryos." *Journal of Anatomy* 137, no. Pt 3: 591–599.

Porro, L. B., C. M. Holliday, F. Anapol, L. C. Ontiveros, L. T. Ontiveros, and C. F. Ross. 2011. "Free Body Analysis, Beam Mechanics, and Finite Element Modeling of the Mandible of *Alligator mississippiensis*." *Journal of Morphology* 272, no. 8: 910–937.

R Core Development Team. 2023. R: A Language and Environment for Statistical Computing. [Computer Software]. R Foundation for Statistical Computing. https://www.r-project.org.

Rolfe, R., K. Roddy, and P. Murphy. 2013. "Mechanical Regulation of Skeletal Development." *Current Osteoporosis Reports* 11: 107–116.

Rot-Nikcevic, I., T. Reddy, K. J. Downing, et al. 2006. "Myf5-/-: MyoD -/- Amyogenic Fetuses Reveal the Importance of Early Contraction and Static Loading by Striated Muscle in Mouse Skeletogenesis." *Development Genes and Evolution* 216: 1-9.

Schlager, S. 2017. "Morpho and Rvcg—Shape Analysis in R: R-Packages for Geometric Morphometrics, Shape Analysis and Surface Manipulations." In *Statistical Shape and Deformation Analysis: Methods, Implementation and Applications*, edited by G. Zhen, S. Li and G. Szekely, 217–256. London, United Kingdom: Academic Press.

Shea, C. A., R. A. Rolfe, and P. Murphy. 2015. "The Importance of Foetal Movement for Co-Ordinated Cartilage and Bone Development in Utero: Clinical Consequences and Potential for Therapy." *Bone & Joint Research* 4, no. 7: 105–116.

Sibonga, J. D., H. J. Evans, H. G. Sung, et al. 2007. "Recovery of Spaceflight-Induced Bone Loss: Bone Mineral Density After Long-Duration Missions as Fitted With an Exponential Function." *Bone* 41, no. 6: 973–978.



Solem, R. C., B. F. Eames, M. Tokita, and R. A. Schneider. 2011. "Mesenchymal and Mechanical Mechanisms of Secondary Cartilage Induction." *Developmental Biology* 356, no. 1: 28–39.

Sullivan, G. 1967. "Abnormalities of the Muscular Anatomy in the Shoulder Region of Paralysed Chick Embryos." *Australian Journal of Zoology* 15: 911–940.

Suominen, H. 2006. "Muscle Training for Bone Strength." Aging Clinical and Experimental Research 18: 85-93.

Tokita, M., and R. A. Schneider. 2009. "Developmental Origins of Species-Specific Muscle Pattern." *Developmental Biology* 331: 311–325.

Watanabe, A., A. C. Fabre, R. N. Felice, et al. 2019. "Ecomorphological Diversification in Squamates From Conserved Pattern of Cranial Integration." *Proceedings of the National Academy of Sciences* 116, no. 29: 14688–14697.

Wolff, J. 1892. Das Gesetz der Transformation der Knochen. Berlin: August Hirschwald Verlag.

Woronowicz, K. C., S. E. Gline, S. T. Herfat, A. J. Fields, and R. A. Schneider. 2018. "FGF and TGF β Signaling Link Form and Function During Jaw Development and Evolution." *Developmental Biology* 444: S219–S236.

Woronowicz, K. C., and R. A. Schneider. 2019. "Molecular and Cellular Mechanisms Underlying the Evolution of Form and Function in the Amniote Jaw." *EvoDevo* 10: 17.

Supporting Information

Additional supporting information can be found online in the Supporting Information section.

